J Sol-Gel Sci Technol
DOI 10.1007/s10971-012-2876-6

ORIGINAL PAPER

The design and characterisation of sol–gel coatings for the controlled-release of active molecules

M. Hernández-Escolano · M. Juan-Díaz · M. Martínez-Ibáñez · A. Jimenez-Morales · I. Goñi · M. Gurruchaga · J. Suay

Received: 29 May 2012 / Accepted: 6 September 2012

Abstract The controlled release of active agents from a matrix has become increasingly important for oral, transdermal or implantable therapeutic systems, due to the advantages of safety, efficacy and patient convenience. Controlled-release hybrid (organic–inorganic) sol–gel coating synthesis has been performed to create a sol with an active molecule included (procaine). Synthesis procedures included acid-catalysed hydrolysis, sol preparation, the addition of a procaine solution to the sol, and the subsequent gelation and drying. The alkoxide precursors used were triethoxyvinylsilane and tetraethyl-orthosilicate (TEOS) in molar ratios of 1:0, 9:1, 8:2 and 7:3. After the determination of the optimal synthesis parameters, the material was physicochemically characterised by silicon-29 nuclear magnetic resonance (^{29}Si-NMR) and Fourier transform infrared spectroscopy, contact angle analysis and electrochemical impedance spectroscopy tests. Finally, the materials were assayed in vitro for their ability to degrade by hydrolysis and to release procaine in a controlled manner. The sustained release of procaine over a 3-day period was demonstrated. A close correlation between release and degradation rates suggests that film degradation is the main mechanism underlying the control of release. Electrochemical analysis reveals the formation of pores and water uptake during the degradation. The quantity of TEOS is one of the principal parameters used to determine the kinetics of degradation and procaine release.

Keywords Sol–gel coatings · Controlled-release · Electrochemical properties

1 Introduction

Controlled-release focuses on delivering biologically active agents locally over extended periods of time [1–4]. The site-specificity of the delivery reduces the potential side-effects that can be associated with the general administration of drugs through oral or parenteral therapy [5]. Prevalent mechanisms for the delivery of biological agents by controlled-release devices are resorption of the drug carrier material and diffusion of the drug [6, 7]. Thus, excellent controlled-release materials are ideally biodegradable with generally good biocompatibility. For the purpose of this paper, we would like to point out that silica-based sol gels can be formulated as resorbable materials with a favourable tissue response [8].

Silica gel obtained by the sol–gel technology is an inorganic or hybrid (organic–inorganic) polymer produced synthetically by the controlled hydrolysis and condensation

M. Hernández-Escolano (✉)
Centro de Biomateriales e Ingeniería Tisular, Universidad Politécnica de Valencia, C. de Vera s/n, 46021 Valencia, Spain
e-mail: miheres@upvnet.upv.es; miheres@doctor.upv.es
URL: http://www.upv.es/cb/

M. Juan-Díaz · M. Martínez-Ibáñez · I. Goñi · M. Gurruchaga
Facultad de Ciencias Químicas, Universidad del País Vasco, P. M de Lardizábal, 3, 20018 San Sebastián, Spain

A. Jimenez-Morales
Departamento de ciencia e ingeniería de materiales e ingeniería química, Universidad Carlos III, Avd. Universidad, 30, 28911 Leganés, Spain

J. Suay
Department of Ingeniería de Sistemas Industriales y Diseño, Universidad de Castellón, Av. Sos Baynat s/n, 12071 Castellón, Spain

Published online: 14 September 2012

of alkoxysilanes. The synthesis of sol–gel silica occurs from liquid precursors ('sol') via the initial formation of 'wet' gels, in which the inorganic network is surrounded by solvents which are later removed to yield a dry material [9]. Depending on the organic polymer chain present in the alkoxysilane the hybrid character of the final material will be defined. This material, originally developed for engineering applications, is currently being studied as a polymer for the entrapment and sustained release of bioactive compounds [10–12]. In contrast to common glass, which is a viscous fluid obtained by the high temperature fusion of SiO_2, sol–gel silica is an amorphous, porous material which is synthesised in mild conditions, which are compatible with the stability of most bioactive compounds. This fact allows its exploitation as a matrix for entrapping bioactive compounds, with several applications already in biotechnology and biomedical sciences.

Radin et al. [13] demonstrated a close correlation between release and degradation rates that suggests that film degradation is the main mechanism underlying the control of release. They also correlated the tailoring of release and degradation properties of the films by controlling sol–gel processing parameters. However the influence of the initial alkoxysilanes selected (the composition of the precursors) in the degradation of the material and its capacity to control the release of active substances has not yet been studied in depth. Aspects such as the type of alkoxylilanes used or the organic content in the final silicon network can be used to design the material according to its capacity to degrade or to tailor the controlled-release of active molecules included in the sol–gel.

The present study reports the synthesis via sol–gel method of hybrid (silica and organic chains) networks with a mixture of two alkoxysilanes VTES and TEOS which can be used as biomaterials as was demonstrated in our research group. Different molar proportions (100–0, 90–10, 80–20 and 70–30) were used. Each one of the compositions has been loaded with a model drug (procaine). The aim of the work is to investigate how changes in composition in the hybrid network influence the degradation of the matrix and further the release of the drug. In order to characterise the network formation, physicochemical analysis was performed (by FTIR and RMN). The electrochemical impedance spectroscopy (EIS) technique was used to study the initial pore structure of the materials and further changes in the coating because of degradation, fundamentally assessing its capacity to resist pore formation and water uptake, recording both parameters as a function of time. Finally, the results of in vitro long-term degradation and controlled-release of procaine are reported and correlated with the physicochemical properties of the different networks.

2 Experimental

2.1 Materials

2.1.1 Sol–gel synthesis

Organic–inorganic hybrid coatings were synthesised from TEOS (Sigma-Aldrich) and VTES (Sigma-Aldrich). The molar ratios were 1:0, 9:1, 8:2, 7:3 = VTES:TEOS. In all cases, 2-propanol was used as a co-solvent to ensure a miscible solution of the siloxanes, the volume ratio of alcohol:siloxane was defined as 1:1 and the stoichiometric amount of acidified water was used as the catalyst of the reaction. The acid–water was prepared by mixing distilled water with 0.1 N HNO_3 to a pH of 1. Solutions were stirred for about 1 h and set for another hour at room temperature before their deposition on Petri dishes by solving casting. This time (2 h) is necessary to ensure the hydrolysis of all of the ethoxy groups.

To obtain coatings with procaine, as it is a water-soluble drug, a 5 % by weight (percent of drug weight to precursor weight) preparation was dissolved in the acidified water to the precursor-alcohol solution to maintain the stoichiometric proportion. The sol–gel protocol synthesis was the same as described above.

2.1.2 Sol–gel coatings

Two types of samples were obtained in order to characterise sol–gel coatings: those deposited on metal and those without a substrate.

Stainless steel AISI 316-L plates (5 × 5 cm, RNSinox, S.L.) were used as a substrate for sol–gel deposition. The plates were cleaned with acetone to remove impurities or oil. A dipping device (KSV instrument-KSV DC) with a controlled withdrawal speed was used for the film deposition. Plates were immersed into the dissolution at a speed of 100 cm min^{-1}, left for 1 min, and the plates were then removed at the same speed.

In order to obtain a free sol–gel film, Teflon moulds were used. An appropriate quantity of sol was poured into the mould to obtain a final dry film thickness of 1 mm.

The coatings were dried and cured using the thermal process described in Table 1. During heating, evaporation

Table 1 Thermal curing applied to the materials and its conditions

Material	TEOS	VTES[a]	V:T
Cure temperature (°C)	50	100	50
Cure time (min)	120	90	120

[a] After cure treatment the samples were dried at 50 °C/15 min and set at the final temperature at 3 °C/min

of the solvents occurred and OH groups condensed to give rise to the final network.

2.2 Chemical characterisation

^{29}Si-NMR solid spectroscopy was used to determine the Si–O–Si cross-linking density after curing treatment. Spectra were recorded on a Bruker 400 AVANCE II spectrometer, equipped with a CP/MAS probe. The samples were placed in a zirconia sample tube. The sample spinning speed at the magic angle to the external field was 5.0 kHz. The ^{29}Si CP MAS-NMR spectra were measured at 59.6 MHz with 10.0 μs ($\pi/2$) pulses, 10 s recycle delays and a 1,500 μs contact time. The signals for about 3,400 pulses were accumulated. The chemical shift is represented in δ (ppm) by convention. Samples were prepared by doping the reaction medium with chromium acetylacetonate as a spin relaxation agent, at a concentration of 2.5×10^{-3} M, to overcome the long relaxation times [14]. Tetramethylsilane was used as an internal reference.

The structure of the hybrid coatings was examined by Fourier-transform infrared (FTIR) spectroscopy (Model FTIR 6700, NICOLET). The spectra were recorded on the attenuated total reflectance (ATR) mode and the wavelength range was between 4,000 and 400 cm^{-1}. For the analysis of the samples, films without a substrate of each precursor and the mixture were prepared.

2.3 Electrochemical impedance spectroscopy (EIS)

Electrochemical impedance spectroscopy tests were carried out on coated samples exposed to 3.5 % NaCl (by weight) in deionised water for up to 24 h. A three electrode electrochemical cell was obtained by sticking a glass cylinder onto the sample sheet and filling it with the test solution. The exposed surface area was 16.6 cm^2. A carbon sheet acted as the counter-electrode and an Ag/AgCl electrode was used as the reference electrode.

The AC impedance data were obtained at the free corrosion potential using an IM6/6eX *Zahner—elektrik* potentiostat and a frequency response analyser. The impedance tests were carried out over a frequency range of 100 kHz down to 10 mHz using a sinusoidal voltage of 10 mV as the amplitude inside a Faraday cage. This was in order to minimise external interferences on the system. The impedance spectra were analysed using Z-view software and two different equivalent circuit models, as shown in Fig. 1. The first model has two time constants with the first corresponding to coating behaviour (R_{po} and C_c) and the second corresponding to interphase (R_p and C_{dl}). The second model has three time constants, with the first referred as the coating response (R_{po} and C_c), the second as the oxide layer (R_{oxid} and C_{oxid}), and the third

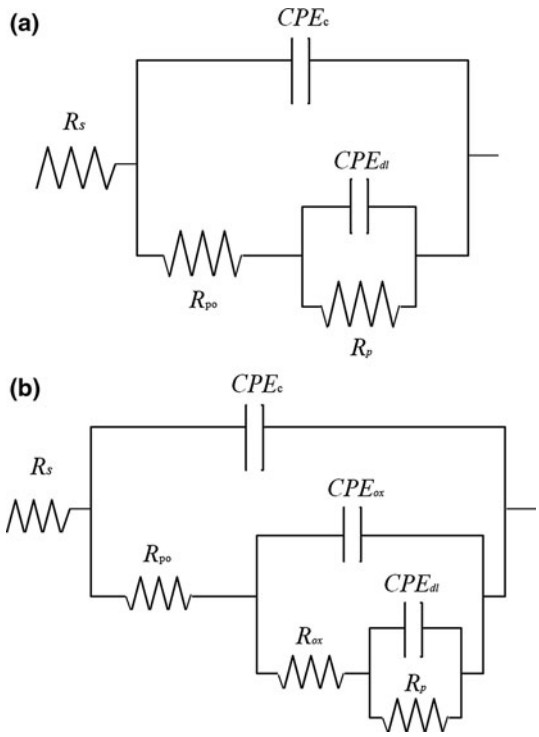

Fig. 1 Equivalent circuit **a** two time constants and **b** three time constants

corresponding to the interphase with metal behaviour (R_p and C_{dl}). The circuit consisted of a working electrode (metal substrate), a reference electrode (Ag/AgCl), electrolyte resistance (R_s), pore resistance (R_{po}), constant phase element of the coating capacitance (CPE_c), oxide layer resistance (R_{oxid}), constant phase element of the oxide layer (CPE_{oxid}), polarisation resistance (R_p) and a constant phase element of the double layer capacitance (CPE_{dl}) [15, 16]. The Chi-squared parameter of the fit was always below 0.01.

Fitting the EIS data to the circuit determines the values of the characteristic parameters of the equivalent circuit, which are generally assumed to be related to the corrosion properties of the system [15, 16]. Fitting the impedance data to the parameters of the first time constant of the circuit (low frequencies) allows the parameters R_{po} and C_c to be obtained. R_{po} can be related to porosity and the deterioration of the coating while C_c is related to the water absorption and coating degradation. R_{oxid} and C_{oxid} are the parameters obtained by fitting the impedance results to the parameters of the second time constant of the circuit (medium frequencies in the case of all three time constants) and referring to the oxide layer properties. Finally, the parameters C_{dl} and R_p are related to the disbonding of the coating and the onset of corrosion at the interface [17–20]. When modelling the equivalent circuit

with CPE, the software gives values of capacitance in sn/Ω units together with a parameter known as "n". When n is close to 1 (ideal capacitor), as was the case in this study, it can be considered that the values of capacitances given by the software match with the effective capacitances (ideal). Thus, it is not necessary to calculate the effective capacitances, and results can be interpreted as capacitances but with sn/′ units instead of those for effective/real capacitances (s/′ or F).

2.3.1 Equivalent circuit interpretation

It is generally assumed that the elements of the equivalent circuits are correlated to the corrosion properties of the system [15, 21–26]. Although it is necessary in order to fit correctly the equivalent circuit to all impedance spectra versus frequency, this study is only related to the characterization of the hydrolysis degradation of the sol–gel coating, and for this reason we will focus our attention to those results obtained at the high frequency where the response of the coating to its exposition to electrolyte (parameters of the equivalent circuit R_{po} and C_c) is located.

The pore resistance R_{po} is a measure of the porosity and deterioration of the coating. R_{po} values have usually been related to the number of pores or capillary channels perpendicular to the substrate surface through which the electrolyte reaches the interface [22]. Although the R_{po} can also increase with immersion time, probably as a result of pore or defect blockage by corrosion products, it usually decreases. Some authors have found three regions in the time dependent decreases of R_{po}. It initially decreases rapidly, then slowly (displaying a plateau) and then again rapidly, coinciding with the appearance of the second semicircle. They explain the plateau by making the assumption that the number of pathways formed is approximately constant with time.

Cc is the capacitance of the coating and it should be a measure of the water permeation into the coating and is given by:

$$C_c = \varepsilon\varepsilon_o A/d \quad (1)$$

where ε is the dielectric constant of the coating, ε_0 the permittivity of vacuum, A the area of the coating exposed to the electrolyte, and d is the thickness. The coating capacitance will usually change (increasing) due to electrolyte absorption because the dielectric constant of water is approximately 5 times greater than that of a typical coating. C_c usually increases at the initial stage of exposure, and it is a measure of water absorption. When the coating has been exposed for a long time it can be correlated to disbonding and deterioration.

2.4 Contact angle

The contact angle of deionised water was determined using an automatic contact angle meter (OCA20 Goniometer). The wettability of the substrates was determined by the half angle method. A sessile drop of 10 µl of deionised water was placed on the coating surface. The value given is the mean value of at least 11 measurements.

2.5 In vitro degradation and release testing

Both degradation and drug release studies were preformed in phosphate buffered saline (PBS) with pH = 6.8 at 37 °C. BS was made from $NaH_2PO_4{\cdot}H_2O$ (Sigma-Aldrich) and $Na_2HPO_4{\cdot}7H_2O$ (Panreac). Hydrolytic degradation was evaluated with the weight loss of samples before and after soaking in PBS. In this case, the samples were prepared without Petri substrate. These samples had a final thickness around 1 mm. After soaked the samples were dried in an oven at 37 °C during 24 h.

In vitro release testing is an established method to test the release kinetics of drugs from solid matrices. The concentration of the various delivered drugs was determined by UV–vis spectrophotometry (Helios-Omega) at maximum absorbance, 291 nm for Pr. Each data point is the average of three individual measurements.

3 Results and Discussion

3.1 Structural characterization

The formation of the sol–gel network depends on the condensation reaction of the Si–OH (obtained by the initial hydrolysis of the alkoxysilanes) to form Si–O–Si bonds. Depending on the extent of the reaction it is possible to obtain more or less open/close networks with different cross-linking degrees. Different conditions were applied in order to obtain good quality coatings (homogeneous and without pores) and those in Table 1 were finally selected.

The VTES and TEOS (pure material) films were studied by ^{29}Si solid RMN after a condensation treatment. The nomenclature followed for the description of the behaviour of the precursors was described extensively in other papers [27–29]. The most useful information from these spectra is the determination of the condensation degree of each precursor used to form the film. Figure 2 shows the solid state Si-NMR spectra of TEOS and VTES.

^{29}Si-RMN solid state spectrum of TEOS coating shows signals associated to Q^2, Q^3 and Q^4. The intensity ratios of these signals indicated a high number of terminal silanol groups, which suggests an incomplete condensation process (Table 2).

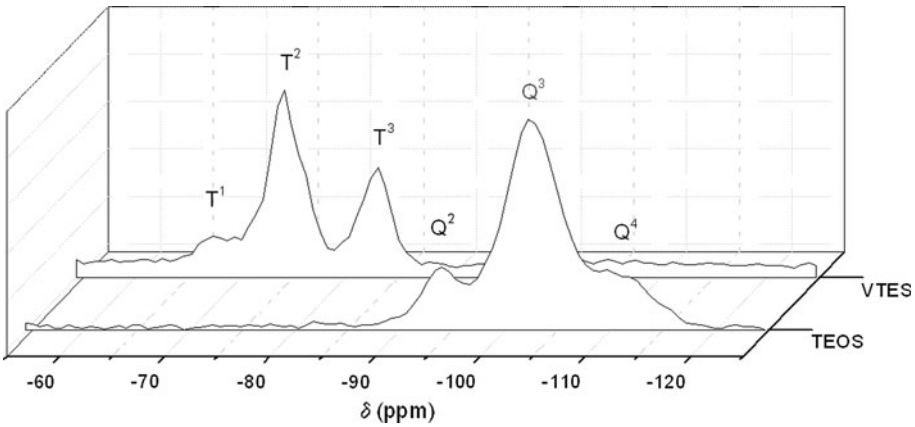

Fig. 2 ^{29}Si solid RMN spectra of TEOS and VTES

The VTES spectrum shows T^1, T^2 and T^3 signals, and the relationship between them indicates that either the vinyl group presence or the curing treatment influenced the cross-linking process giving rise to a partially open network in which the silanol groups remain unreacted (Table 2).

Films from precursor mixtures (9VTES-1TEOS, 8VTES-2TEOS, 7VTES-3TEOS) were prepared and the 7VTES-3TEOS sample was studied by ^{29}Si solid RMN (Fig. 3).

The spectra shows T^2 and T^3 species from VTES and Q^3 and Q^4 from TEOS, indicating the culmination of the condensation process during the curing treatment. The signals corresponding to VTES in the mixture had a peak intensity relationship for T^2/T^3 of 61/39 indicating that there were still Si–OH groups able to react, but this was less than in the case of the material obtained only with VTES. In the case of the signals corresponding to TEOS in the mixture, the peak intensity relationship of Q^3/Q^4 was 17/83 indicating that the silicon atoms of this type of molecule have a very high level of condensation under the applied curing conditions (Table 2).

It can be concluded, therefore, that the network formed in the case of mixtures (at least in the case of 7V-3T) has a larger condensation index for each silicon atom than in the case of using pure materials (from VTES or TEOS), even when using more severe curing conditions. For this reason, the quantity of Si–OH groups in the mixture will be lower than in the pure materials.

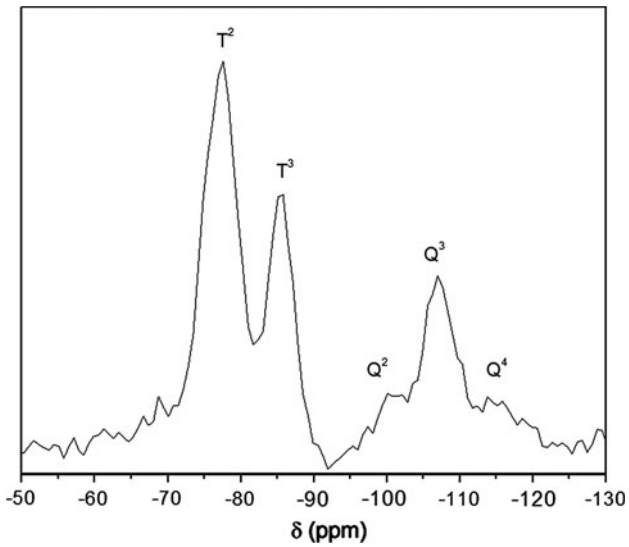

Fig. 3 ^{29}Si solid RMN spectra of VTES:TEOS molar ratio 7:3

The FTIR assay was used to study the polysiloxanic network (Si–O–Si) formed from the different mixtures of alkoxysilanes (VTES, 9VTES-1TEOS, 8VTES-2TEOS and 7VTES-3TEOS).

Figure 4 shows the FTIR spectra of the films obtained with VTES and 7V:3T. Both spectra have bands associated with the vibration of chains Si–O–Si around 1,075, 1,163 and 800 cm^{-1}, which are characteristic of the formation of a polysiloxanic network [30, 31]. The addition of TEOS did not reveal clear changes in the FTIR spectra of the materials, and only made a relative increase of intensity of

Table 2 ^{29}Si chemical shift in solid of samples TEOS, VTES, VTES:TEOS molar ratio 7:3

	^{29}Si chemical shift (δ/ppm)						Peak intensity proportion	
	Q^2	Q^3	Q^4	T^1	T^2	T^3	$Q^2/Q^3/Q^4$	$T^1/T^2/T^3$
TEOS	−93	−102	−109	–	–	–	18/66/17	–
VTES	–	–	–	−57	−74	−82	–	11/57/32
7V:3T		−101	−107		−77	−85	17/83	61/39

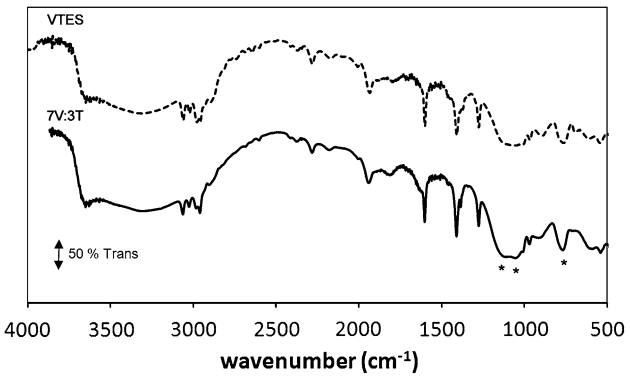

Fig. 4 FTIR spectra (4,000–400 cm^{-1}) of VTES and VTES:TEOS (molar ratio 7:3)

these peaks. In both spectra, the bands associated with the vibration of OH species (3,300–3,500 cm^{-1}), and Si–OH terminals (3,740 cm^{-1}) [30, 31] can be seen. Additionally, bands associated with the vinyl group of VTES are detected at wavelengths of 3,060, 1,600 and 1,450 cm^{-1}, corresponding to $=CH_2$, C=C and Si–C, respectively. Networks formed from VTES have a higher organic character because of the vinyl group. The inorganic character of the network increases with TEOS content.

The conclusion is that the synthesis conditions and the curing parameters applied to the systems have been correctly selected in order to obtain, in all cases, polysiloxane networks with the presence of vinyl organic chains in the materials.

3.2 Wettability

The contact angle was measured on coatings with different TEOS contents (VTES, 9V:1T, 8V:2T and 7V:3T) applied on AISI 316L steel plates with the cure treatment described above. The contact angle values obtained are presented in Table 3.

The VTES coating has a hydrophobic character with a contact angle of 80°. The addition of 10 % TEOS (9V:1T) did not influence the contact angle value. However, larger additions (20 and 30 % TEOS) caused a significant increase in the hydrophilicity, giving rise to contact angle values around 70° and 55°, respectively.

By analysing the RMN results it can be deduced that the presence of TEOS in the formulations reduces the number of silanol groups (Si–OH), so differences in contact angle values have to be correlated with the presence of the organic group (vinyl) and the content of Si–O–Si bonds in the network. It is well known that the presence of the vinyl group makes the coating hydrophobic. As a result, additions of more than 10 % of TEOS can make the coatings much more hydrophilic due to their final inorganic structure [32]. Therefore, the design of the hydrophilic-hydrophobic character of the coating can be performed by initially selecting the appropriate mixture of the alkoxysilanes.

Table 3 Contact angle measures for VTES, 9V:1T, 8V:2T and 7V:3T applied on stainless steel

Material	VTES	9V:1T	8V:2T	7V:3T
Contact angle (°)	80.1 ± 0.5	80.4 ± 1.4	69.4 ± 0.5	55.5 ± 1.0

3.3 EIS

The EIS test was performed to study the coating properties (the creation of pores and water uptake) along the time to the electrolyte of VTES, 9V:1T, 8V:2T and 7V:3T samples obtained by dip-coating on stainless steel AISI 316L plates.

Figure 5 shows the Nyquist graph of the impedance evolution with time over first 24 h for VTES, 9V:1T, 8V:2T and 7V:3T.

Impedance spectrum shows that VTES's impedances values are bigger than those obtained in coatings with TEOS content. As the quantity of TEOS increases the impedance module decreases. The exposure to electrolyte has a limited response in the case of VTES which means there are not clear changes in the material during the time of the test, while in coatings with TEOS the behavior is the opposite. There are big changes in the impedance with the exposure to electrolyte that would be correlated to the phenomena of degradation.

In order to analyse the behaviour of the coatings, the impedance spectra were modelled using equivalent circuits, as shown in Fig. 1. In the case of VTES coatings, only two time constants were detected in the impedance response, while three time constants were detected for coatings in the presence of TEOS. The presence of an oxide layer in the case of TEOS coatings could be due to a higher permeability of these coatings, which was reflected by the significant decrease of the impedance value.

Figure 6 shows the impedance experimental results for the 7V:3T coating at an exposition time of 0 h and the impedance results modelled according to the circuit with three time constants. A good fit was obtained for all coatings over the complete range of frequencies.

As this study tried to understand how the electrolyte exposure affects the material degradation, the discussion will be focused on the first time constant parameters, which are related to the coating behaviour.

Figure 7 shows pore resistance and coating capacity parameters obtained from the response at high frequencies of all coatings.

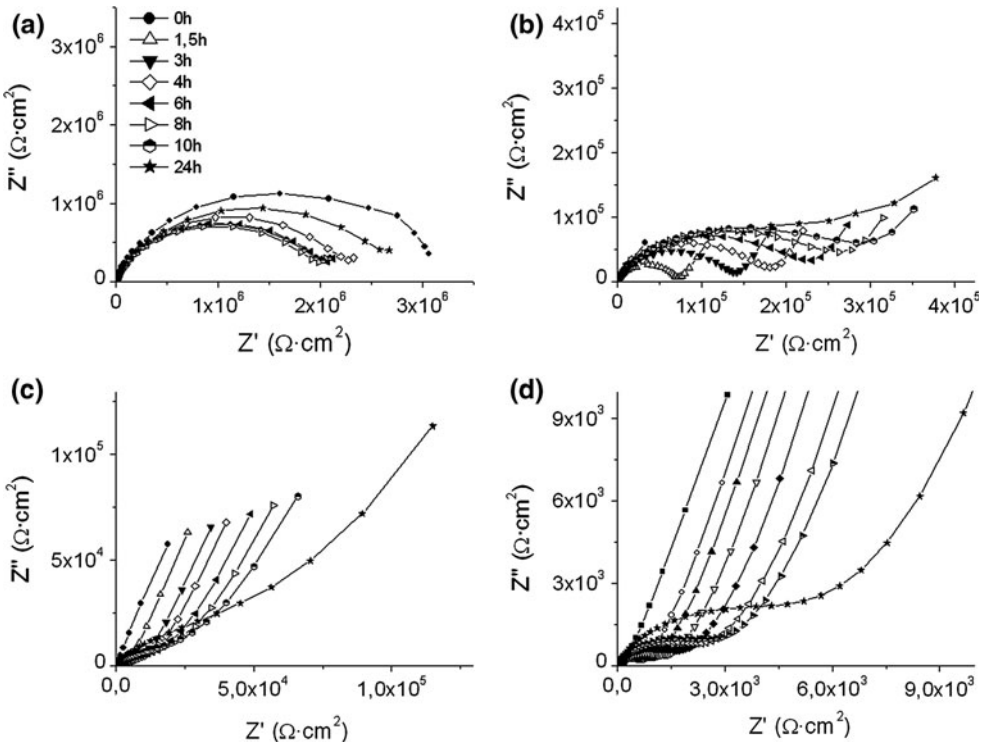

Fig. 5 Evolution of Nyquist plot for **a** VTES, **b** 9V:1T, **c** 8V:2T and **d** 7V:3T coatings during 24 h immersion in electrolyte (deionized water with 3.5 % NaCl by weight)

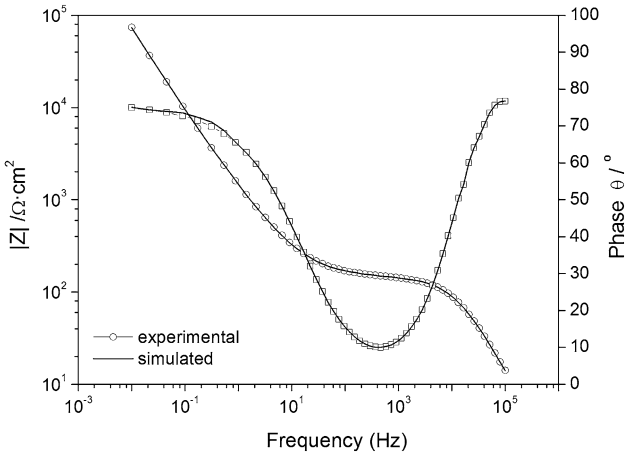

Fig. 6 Bode plot with experimental and simulated points obtained for 7V:3T coating before 0 h of immersion in electrolyte (deionised water with 3.5 % NaCl by weight)

The R_{po} value is a measure of the ionic resistance through the pores of the coatings and is inversely proportional to the extent and number of defects in the coating. The evolution of R_{po} with the exposure time in the electrolyte gives information about the coating capacity to avoid the formation of pores across the film due to its degradation. High and constant R_{po} values are attributed to coatings which do not degrade during electrolyte exposure. It can be clearly seen in Fig. 7 that coatings with TEOS content have values of R_{po} that are two orders of magnitude below those observed for VTES. Coatings with TEOS showed high hydrophilicity (especially 8V:2T and 7V:3T), offering no resistance to the flow of water through the coating. This last factor, combined with the degradation of the Si–O–Si bond (with a bigger proportion in these networks) by hydrolysis, explains the results obtained. The increase in the resistance value with time, in coatings with 20 and 30 % of TEOS, can be explained by the process of pore blockage due to the formation of an oxide layer induced by the high permeability of the coatings.

The increase in the value of C_c can be correlated using Eq. (1) with an increase in the permittivity ε value, with the rest of parameters remaining constant for a specific coating sample and test. As a result, an increase of permeability is directly related to an increase of water content in the coating. As seen in VTES sample, C_c values are low (10^{-8} F cm^{-2}) and constant over the time. As the TEOS content increases C_c values are larger than for VTES, and in all cases they increase with exposure time. Therefore, the water amount and the rate of absorption in the coating is higher as the TEOS content increases, which is more noticeable in formulations with a TEOS content that is higher than 20 %.

The water is able to penetrate the coatings formulated with TEOS (in a manner that is directly correlated with its quantity) possibly because of hydrophilicity. The number of pores increases with the exposure time showing a possible effect of Si–O–Si bond degradation by hydrolysis.

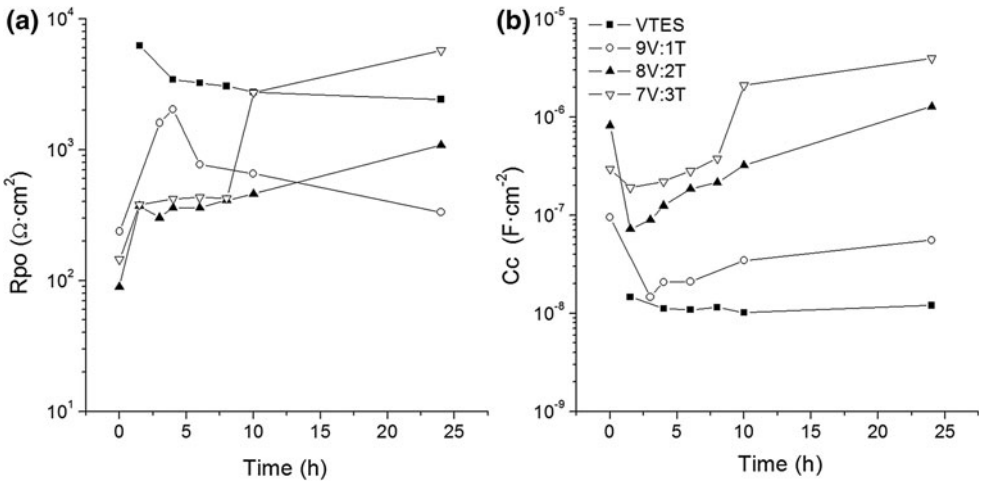

Fig. 7 Evolution of **a** pore resistance Rpo and **b** coating capacitance Cc versus time of exposure to electrolyte (deionised water with 3.5 % NaCl by weight) for VTES, 9V:1T, 8V:2T and 7V:3T applied on AISI 316L

3.4 Degradation

The dissolution of various forms of solid silica in aqueous solutions has been the focus of several studies [33]. It has been established that any form of solid silica in contact with aqueous solutions dissolves into monosilicic acid ($Si(OH)_4$) through hydrolysis, which can be expressed as follows:

$$SiO_2(s) + 2H_2O \leftrightarrow Si(OH)_4(aq) \quad (2)$$

The weight loss of samples (n = 3) of VTES, 9V:1T, 8V:2T and 7V:3T is represented as a function of immersion time (up to 6 weeks) in Fig. 8.

The data indicated that the degradation was gradual and sustained during the full duration of the degradation test. The degradation amount and the kinetic are composition-dependent. VTES samples showed a very low initial degradation (first week) of about 3 % of the weight and this reached a steady state the rest of the time.

As the percentage of TEOS in the composition is higher, the initial degradation increased up to 12 % and reached the steady state after 3 weeks. There was a large change of the degradation kinetics when only 10 % of TEOS was added, and increments up to 30 % of TEOS did not introduce large kinetic changes. However, when there was a higher TEOS content in the composition there was more degradation in the material.

These degradation results are well correlated with results obtained in the hydrophilicity and electrochemical parameters. As TEOS content increases the resistance to water-flow through a material is reduced and the water content increases forming new pores. As a consequence, water can produce the hydrolysis in the network breaking the Si–O–Si bonds.

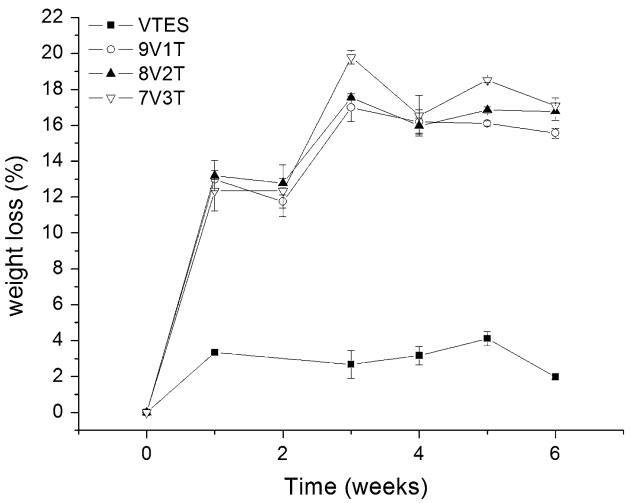

Fig. 8 Hydrolytic degradation (weight loss) versus time of exposure to PBS at 37 °C for VTES, 9V:1T, 8V:2T and 7V:3T

3.5 Procaine control releases

Figure 9 shows the release curves as a function of TEOS content (VTES, 9V:1T; 8V:2T and 7V:3T) when 5 % of procaine was added. The test was performed at 37 °C with a pH of 6.8 across 3 days. In the graph, M_t/M_∞ versus time is represented, where M_t is the quantity of drug detected at a specific time (t) and M_∞ is the quantity of drug incorporated in the material.

The VTES material shows a slow release, reaching 5 % in the first 5 h. At the end of the test, only 10 % of the drug incorporated in the material had been delivered.

The addition of TEOS in the formulation changes the release kinetics, as procaine release increases with the TEOS content. The procaine release kinetics show a first rapid release during the first 24 h, which could be due to the drug being incorporated in the pores that are in contact with the medium, followed by a slower release of the drug present in the inner parts of the material [34].

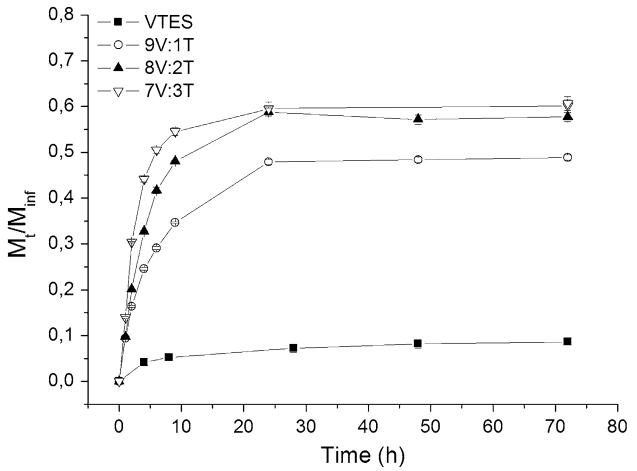

Fig. 9 Comulative procaine release versus versus time of exposure to PBS at 37 °C for VTES, 9V:1T, 8V:2T and 7V:3T

The TEOS incorporation produces a significant change in the physicochemical properties of the material, making it more hydrophilic and degradable. The water uptake is higher and the porosity of the material increases. Since the procaine is very soluble in water its release can be controlled either by the amount added to the film or by the degradation of the material. Therefore, the chemical composition of the sol–gel material and in particular the quantity of TEOS incorporated in the formulation can be used to design the release kinetics.

4 Conclusions

This study demonstrated that sol–gel coatings could be used as drug controlled-release systems. The data suggest that changes in the sol–gel formulation, as a result of varying the TEOS content, allow the variation of the drug release. With an increase in TEOS content the hydrophilicity and the water absorption of the coating grew, due to a decrease of the organic character of the hybrid material. The presence of TEOS, which is a silicon precursor that can form four siloxane bridges, increased the Si–O–Si density. Moreover, polysiloxane networks have high degradability in contact with water, allowing a high drug release. As a result, TEOS content is a crucial parameter for determining drug release kinetics. Therefore, sol–gel coatings can be used as a promising drug delivery system that can be applied to metallic implants in order to reduce the side-effects associated with oral drug administration.

Acknowledgments The supports of the Spanish Ministry of Economy and Competitiveness through project IPT-010000-2010-004 and of the University of the Basque Country (UPV/EHU) through "UFI11/56" are kindly acknowledged. We are especially thankful to D. Antonio Coso and the personal of his company (Ilerimplant S.L www.ilerimplant.com) for their cooperation.

References

1. Alias J, Silva I, Goñi I, Gurruchaga M (2008) Hydrophilic amylose-based graft copolymers for controlled protein release. Carbohydr Polym 74(1):31–40
2. Silva I, Gurruchaga M, Goñi I (2009) Physical blends of starch graft copolymers as matrices for colon targeting drug delivery systems. Carbohydr Polym 76(4):593–601
3. Echeverria I, Silva I, Goni I, Gurruchaga M (2005) Ethyl methacrylate grafted on two starches as polymeric matrices for drug delivery. J Appl Polym Sci 96(2):523–536
4. Castellano I, Goni I, Ferrero M, Munoz A, Jimenez-Castellanos R, Gurruchaga M (1999) Synthetic PMMA-grafted polysaccharides as hydrophilic matrix for controlled-release forms. Drug Dev Ind Pharm 25(12):1249–1257. doi:10.1081/ddc-100102295
5. Langer R, Peppas NA (2003) Advances in biomaterials, drug delivery, and bionanotechnology. AIChE J 49(12):2990–3006
6. Ibim SM, Uhrich KE, Bronson R, El-Amin SF, Langer RS, Laurencin CT (1998) Poly(anhydride-co-imides): in vivo biocompatibility in a rat model. Biomaterials 19(10):941–951
7. Gombotz WR, Pankey SC, Bouchard LS, Phan DH, Puolakkainen PA (1994) Stimulation of bone healing by transforming growth factor-beta1 released from polymeric or ceramic implants. J Appl Biomater 5(2):141–150
8. Radin S, Ducheyne P (2004) Nanostructural control of implantable xerogels for the controlled release of biomolecules. In: Reis R.L, Weiner S (eds) Learning from nature how to design new implantable biomaterials: from biomineralization fundamentals to biomimetic materials and processing routes, Proceedings of the NATO advanced study institute, Alvor, Algarve, Portugal, 13-24 October 2003. NATOScience Series II: Mathematics, Physics and Chemistry, vol 171, pp 59–74
9. Teoli D, Parisi L, Realdon N, Guglielmi M, Rosato A, Morpurgo M (2006) Wet sol-gel derived silica for controlled release of proteins. J Controlled Release 116(3):295–303
10. Jin W, Brennan JD (2002) Properties and applications of proteins encapsulated within sol-gel derived materials. Anal Chim Acta 461(1):1–36
11. Bottcher H, Slowik P, Suss W (1998) Sol-gel carrier systems for controlled drug delivery. J Sol Gel Sci Technol 13(1–3):277–281. doi:10.1023/a:1008603622543
12. Radin S, Chen T, Ducheyne P (2009) The controlled release of drugs from emulsified, sol gel processed silica microspheres. Biomaterials 30(5):850–858
13. Radin S, Ducheyne P (2007) Controlled release of vancomycin from thin sol-gel films on titanium alloy fracture plate material. Biomaterials 28(9):1721–1729
14. Jitianu A, Britchi A, Deleanu C, Badescu V, Zaharescu M (2003) Comparative study of the sol–gel processes starting with different substituted Si-alkoxides. J Non Cryst Solids 319(3):263–279
15. García SJ, Suay J (2006) Anticorrosive properties of an epoxy-Meldrum acid cured system catalyzed by erbium III trifluromethanesulfonate. Prog Org Coat 57(4):319–331
16. García SJ, Suay J (2009) Optimization of deposition voltage of cataphoretic automotive primers assessed by EIS and AC/DC/AC. Prog Org Coat 66(3):306–313
17. Amirudin A, Thieny D (1995) Application of electrochemical impedance spectroscopy to study the degradation of polymer-coated metals. Prog Org Coat 26(1):1–28
18. Walter GW (1981) Application of impedance measurements to study performance of painted metals in aggressive solutions. J Electroanal Chem Interfacial Electrochem 118:259–273
19. Walter GW (1986) A review of impedance plot methods used for corrosion performance analysis of painted metals. Corros Sci 26(9):681–703

20. Tang N, van Ooij WJ, Górecki G (1997) Comparative EIS study of pretreatment performance in coated metals. Prog Org Coat 30(4):255–263
21. van Westing EPM, Ferrari GM, de Wit JHW (1993) The determination of coating performance with impedance measurements-I. Coating polymer properties. Corros Sci 34(9):1511–1530
22. Rodríguez MT, Gracenea JJ, García SJ, Saura JJ, Suay JJ (2004) Testing the influence of the plasticizers addition on the anticorrosive properties of an epoxy primer by means of electrochemical techniques. Prog Org Coat 50(2):123–131
23. García SJ, Suay J (2006) Application of electrochemical techniques to study the effect on the anticorrosive properties of the addition of ytterbium and erbium triflates as catalysts on a powder epoxy network. Prog Org Coat 57(3):273–281
24. García SJ, Rodríguez MT, Izquierdo R, Suay J (2007) Evaluation of cure temperature effects in cataphoretic automotive primers by electrochemical techniques. Prog Org Coat 60(4):303–311
25. García SJ, Suay J (2007) A comparative study between the results of different electrochemical techniques (EIS and AC/DC/AC): application to the optimisation of the cataphoretic and curing parameters of a primer for the automotive industry. Prog Org Coat 59(3):251–258
26. Garcia SJ, Suay J (2007) Epoxy powder clearcoats used for anticorrosive purposes cured with ytterbium III trifluoromethanesulfonate. Corrosion 63(4):379–390
27. Méndez-Vivar J, Mendoza-Bandala A (2000) Spectroscopic study on the early stages of the polymerization of hybrid TEOS–RSi (OR′)3 sols. J Non Cryst Solids 261(1–3):127–136
28. Lippmaa E, Samoson A, Mägi M, Teeäär R, Schraml J, Götz J (1982) High resolution 29Si NMR study of the structure and devitrification of lead-silicate glasses. J Non Cryst Solids 50(2): 215–218
29. Magi M, Lippmaa E, Samoson A, Engelhardt G, Grimmer AR (1984) Solid-state high-resolution Si29 chemical-shifts in silicates. J Phys Chem 88(8):1518–1522
30. Almeida RM, Marques AC (2005) Characterization of sol-gel materials by infrared spectroscopy. In: Sumio S (ed) Sol-gel science and technology. Processing, characterization and applications, vol II characterization of sol-gel materials and products. Kluwer, Lisboa, pp 65–89
31. Innocenzi P, Brusatin G, Guglielmi M, Babonneau F (2005) Structural characterization of hybrid organic-inorganic materials. In: Sumio S (ed) Sol-gel science and technology. Processing, characterization and applications, vol II characterization of sol-gel materials and products. Kluwer, Lisboa, pp 139–157
32. Zolkov C, Avnir D, Armon R (2004) Tissue-derived cell growth on hybrid sol-gel films. J Mater Chem 14(14):2200–2205
33. Falaize S, Radin S, Ducheyne P (1999) In vitro behavior of silica-based xerogels intended as controlled release carriers. J Am Ceram Soc 82(4):969–976
34. Bottcher H (2000) Bioactive sol-gel coatings. Adv Synth Catal 342(5):427–436